

## Photoemission spectra and band structures of simple metals

Kenneth W.-K. Shung\* and G. D. Mahan

*Solid State Division, Oak Ridge National Laboratory, Oak Ridge, Tennessee 37831  
and Department of Physics, University of Tennessee, Knoxville, Tennessee 37996*

(Received 31 August 1987)

We present a detailed calculation of the angle-resolved photoemission spectra of Na. The calculation follows a theory by Mahan, which allows for the inclusion of various bulk and surface effects. We find it important to take into account various broadening effects in order to explain the anomalous structure at  $E_F$ , which was found by Jensen and Plummer in the spectra of Na. The broadening effects also help to resolve the discrepancy of the conduction-band width. Efforts are made to compare our results with new measurements of Plummer and Lyo. We discuss the ambiguity concerning the sign of the crystal potential and comment on charge-density waves in the systems. We have also generalized our discussions to other simple metals like K.

### I. INTRODUCTION

In the past few years, there has been very active research on angle-resolved photoemission spectra of simple metals.<sup>1-6</sup> These studies are interesting because they enable us to examine the band structure of these materials, which is generally regarded to be well described by a nearly-free-electron (NFE) model. Therefore, analysis of the spectra can tell us if the NFE model is valid. Moreover, because of the simplicity of the simple metal's band, we can closely study photoemission processes without interference from complicated electronic band structures.

Figure 1 demonstrates the NFE bands of Na in the [110] direction. In drawing this diagram, we have elevated the conduction band according to the applied photon energy ( $\hbar\omega$ ), so that the intersecting points  $P$  and  $P'$  correspond to photoexcitations at  $\hbar\omega=24$  and 33 eV, respectively. Such excitations satisfy both the energy and the momentum conservation:

$$E(\mathbf{k} + \mathbf{G}) = E(\mathbf{k}) + \hbar\omega, \quad (1)$$

where  $\mathbf{G}$  is a reciprocal-lattice vector. According to this relation, the conduction band  $E(\mathbf{k})$  can be easily traced out by measuring the photoelectrons at various photon energies. It should be noticed that for  $\hbar\omega=33$  eV (i.e.,  $P'$  in Fig. 1), the transition, although it satisfies Eq. (1), is forbidden because the initial state is not occupied. Therefore, if the NFE model describes the system correctly, it predicts a gap at  $31.7 < \hbar\omega < 37.9$  eV, where no photocurrent could be generated.

The simple picture presented above according to Eq. (1) was found by Jensen and Plummer (JP) to be incompatible with their measurement.<sup>3</sup> The discrepancies between the NFE theory and the measurement are the following. First, JP found that at the expected gap region there actually appears a stationary narrow peak that corresponds to initial states at the Fermi level. This result was regarded as evidence that the band close to  $E_F$  (the Fermi energy) is severely distorted, and hence that charge-density waves (CDW's) exist in the system.<sup>5</sup> Second, besides the vertical transitions which satisfy Eq.

(1), there are important contributions due to momentum nonconserving transitions. Such nonvertical transitions form an edge structure at  $E(\mathbf{k})=E_F$  in the spectra (see Fig. 2 of Ref. 3). Third, the measured bandwidth is  $2.5 \pm 0.1$  eV, instead of the 3.2 eV which is predicted by the NFE theory. Such large band narrowing cannot be entirely accounted for by many-body calculations,<sup>7</sup> which predict  $\sim 0.3$ -eV narrowing of the width due to the energy dependence of the electron self-energy. JP, therefore, concluded that their results show clear inaccuracies in the many-body theory, and they suggested that significant corrections for many-body effects are needed

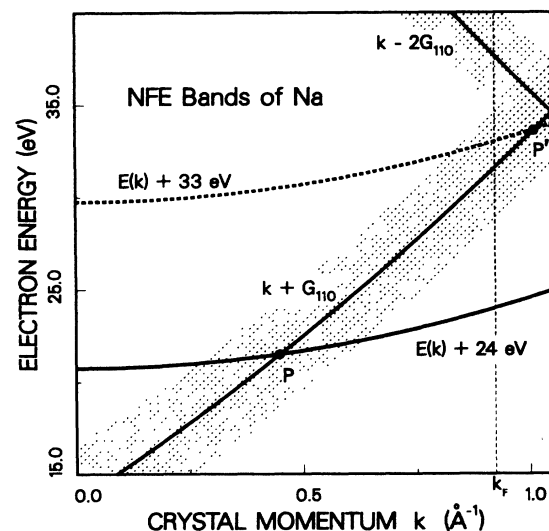


FIG. 1. The NFE bands of Na are shown in which the conduction band has been elevated by the applied photon energies of 24 eV (the solid curve) and 33 eV (the dashed curve), respectively. The intersections  $P$  and  $P'$  correspond to the vertical transitions in photoemission at the given photon energies. The shaded curves represent the broadened final states.

in band calculations.

In a recent calculation<sup>6</sup> (to be referred to as I), Shung and Mahan showed that the discrepancies which we listed above can be explained with a NFE band structure. The calculation was based on a theory of angle-dependent photoemission by Mahan,<sup>8</sup> in which various bulk and surface effects can be treated on an equal footing. It was found that the key to the problem is that the excited electrons have a finite mean free path (MFP) because of Coulomb scattering, or that the electron states have a finite width as is shown in Fig. 1. This fact not only broadens the spectra, it also relaxes the strict momentum conservation of Eq. (1). Basically, this effect explains, according to our theory, both the appearance of the edge structure at photon energies outside of the gap, and the presence of the stationary peak within the gap. Take Fig. 1, for example; although the transition at  $P'$  is forbidden, photoexcitations are still possible at  $\hbar\omega = 33$  eV for those conduction electrons which intersect the broadened bands in the final states. This paper, as a complement of I, provides more details of the calculation. We also include results for K—the spectra of which are found to be similar to that of Na.

As to the conduction-band width, it was argued in I that various broadening effects could explain part of the observed reduction. In the present work, we will include the broadening of the initial states, which was neglected in I. This broadening effect, together with other effects (e.g., the interference) is found to cause a bandwidth reduction of 0.2–0.4 eV in the photoemission spectra of Na. This reduction due to the broadening, together with the many-body effect, seems to provide a satisfactory explanation of the observed bandwidth of Na. Discrepancies are also found in the bandwidth of other materials,<sup>1–4</sup> which probably can be explained by the same broadening effect.

In short, our calculation strongly suggests that the conduction band of Na (and possibly other simple metals too) can be very well described by a NFE model. This result disagrees sharply with the theory of CDW's, which predicts a severe band distortion at  $E_F$ . We will further comment on the CDW's in Na later in this paper. The calculation also shows that the NFE bandwidth, after being modified for many-body effects, is fairly close to JP's results. We emphasize the importance of various broadening and surface effects in photoemission processes. These effects are expected to be important in photoemission in general.

The remaining part of the paper is organized as follows. Section II contains the theory which describes photoemission processes, and which is presented in a form ready for evaluating the spectra. The calculated results and discussions are given in Sec. III. In Sec. IV we extend our discussions to new experimental results of Plummer and Lyo.<sup>9</sup> There we stress the importance of self-energy shifts of electronic states, and we argue that surface Bragg reflection might explain the observed azimuthal-angle dependence in photoemission spectra. A discussion on the sign of the crystal potential and a comment on CDW's are also included therein. Concluding remarks are finally summarized in Sec. V.

## II. THEORY

This calculation, as was stated in the Introduction, closely follows a photoemission theory of Mahan.<sup>8</sup> In the theory, photoemission is considered an inelastic-scattering process and the quantity to be calculated is the emitted current per solid angle per energy,  $d^2I/d\Omega dE$ . For normal emission, which is the case of JP's measurement, we have formulated the result in I. In the following, we will modify it for more generalized cases of near-normal emissions.

The requirement that momentum parallel to the surface be conserved is expressed by the relation

$$p_{\parallel} = k_{i\parallel} + G_{\parallel} , \quad (2)$$

where  $p_{\parallel} = (2mE)^{1/2} \sin\theta$ ,  $\theta$  is the angle of emission measured from the norm of the surface, and  $E = p^2/2m$  is the energy of the emitted electron measured externally. When the applied photon energy is not too high,  $p_{\parallel}$  is small at small-angle emissions. In simple metals,  $G_{\parallel}$  is either zero or greater than  $\sim 2k_F$ . Hence, as long as  $p_{\parallel} < k_F$ ,  $G$  must vanish in Eq. (2). In such cases, as well as in the case of normal emissions,<sup>6</sup> Mahan's theory reduces to a simple one-dimensional integration:<sup>8</sup>

$$\frac{d^2I}{d\Omega dE} = \frac{em}{2\pi^2} \int_0^{k_{m\perp}} dk_{i\perp} p |M(p, k_i)|^2 \times \delta(E \cos^2\theta - E(k_{i\perp}) - \hbar\omega + V_0) , \quad (3)$$

where the upper limit  $k_{m\perp}$  equals  $(k_F^2 - p_{\parallel}^2)^{1/2}$  and becomes  $k_F$  if  $\theta = 0$ .  $M(p, k_i)$  is the excitation matrix element, which we will discuss later.  $E(k_{i\perp})$  is the perpendicular part of the initial-state energy. The  $\delta$  function in Eq. (3) specifies the energy conservation in a form slightly different from Eq. (1) due to the introduction of the surface barrier  $V_0$ , which the photoelectron must overcome to reach the outside. This expression obviously reduces to Eq. (1) of I in the  $\theta = 0$  case, as it should. Corresponding to JP's measurement on Na, where  $\hbar\omega < 100$  eV we have estimated that Eq. (3) is applicable for  $\theta$  less than  $10^\circ$ .

In order to evaluate Eq. (3), we need to specify the excitation matrix element  $M(p, k_i)$ . The treatment of this part is the same as in I and is included here for completeness. We first notice that photon fields do not interact with a homogeneous electron system.<sup>10</sup> In other words, photoemission may take place only due to inhomogeneities in the system. In the calculation, we take into account those effects from the surface potential  $V_s(z)$ , and from the crystal potential  $V_c(z) = \sum_G V_G \exp(-iGz)$ , where  $G$ 's are perpendicular to the surface (i.e., along the  $z$  axis). We thus get<sup>8</sup>

$$M(p, k_i) = F(\omega) \int dz \phi^>(p, z) \times \left[ \left[ -\frac{\partial}{\partial z} \right] [V_s(z) + V_c(z)] \right] \times \phi(k_i, z) , \quad (4)$$

where  $|F(\omega)|^2 \propto \omega^{-3}$ .  $\phi(k_i, z)$  is the initial-state wave function and  $\phi^>(p, z)$  is an in-going wave which contains a factor describing the scattering by the surface (see Ref. 8). It should be noticed that higher-order effects due to the surface and to the bulk can be included in  $M(p, k_i)$  in Mahan's theory, although we find that Eq. (4) contains major features which appear in the spectra.

It is clear that the calculation of photoemission spectra now hinges on the determination of  $\phi(k_i, z)$  and  $\phi^>(p, z)$ . As was noted by Mahan,<sup>8</sup> once the surface potential is given, both  $\phi$  and  $\phi^>$  can be determined by solving a one-dimensional Schrödinger's equation. At this juncture, it is important to notice that the MFP of out-going electrons is short [4–6 Å at ~30 eV (Ref. 11)]. Only photoelectrons created in the surface region can come out of the solid, and hence details of the potential in the surface region are very important in this problem. It is, therefore, as we emphasized in I, necessary to use a realistic potential to describe the surface and, meanwhile, to appropriately include decay mechanisms of electrons. If we approximate the metal surface by a step function, we can easily express Eq. (3) in analytical forms.<sup>8</sup> Such results are illustrative but not accurate for real metals. We find that step potentials lead to overestimation of the surface effects.

In our calculation, the effects of the crystal potential on the electronic energies are neglected. For the spectra of Na and K, this approximation is valid since the effects are small. It has been calculated that the shift of the Fermi energy due to the crystal potential is  $-0.06$  eV ( $-0.07$  eV) for Na (K).<sup>8</sup> However, for some other simple metals, e.g., Li (Ref. 8) and Be (Ref. 2), the effects of the crystal potential are strong. For these metals, it would be important to include the crystal potential effect when calculating their spectra. It should also be pointed out that, by neglecting the band-structure effect, the NFE bands are spherically symmetric. Consequently, the angle-dependent spectra are expected to be symmetric about the  $z$  axis, as is clear from Eqs. (3) and (4), i.e., it is independent of the azimuthal angle of emission. However, a recent measurement reveals that there is asymmetry in the azimuthal angle of Na spectra. Later in Sec. IV we will discuss, still within the NFE model, a possible explanation of this anisotropy in photoemission.

For simple metals like Na, the best available surface potential is given by a calculation of Lang and Kohn (LK),<sup>12</sup> in which the potential is determined self-consistently via the density-functional theory. We use LK's potential as input, and evaluate  $\phi(k_i, z)$  and  $\phi^>(p, z)$  numerically.

The wave functions obtained above need to be modified so that the finite MFP of electrons can be accounted for. For this purpose, we have evaluated<sup>13</sup> the self-energy of electrons,

$$\Sigma(k, E(k)) = \Sigma_1(k, E(k)) + i\Sigma_2(k, E(k)), \quad (5)$$

by applying the Rayleigh-Schrödinger perturbation theory, and can thus drop the energy dependence of the self-energy.<sup>8</sup> The real part  $\Sigma_1(k)$  accounts for energy shifts of the electronic states and results in the bandwidth narrowing. The inverse of the imaginary part of the self-

energy represents the electron's lifetime, and the distance an electron travels during the lifetime is its MFP. The mechanism of electron decay is Coulomb scattering, and our calculation is basically the same as that of Quinn.<sup>14</sup> The calculated results for both the MFP and  $\Sigma_2(k)$  are shown in Fig. 2 for both Na and K. These theoretical values are in fairly good agreement with measurements.<sup>11</sup> We include such decay factors in our calculation by modifying  $\phi^>$ :

$$\phi^>(p, z) \rightarrow \phi^>(p, z) \exp[-z/2\lambda(k)] \quad \text{if } z > 0, \quad (6)$$

where we have assumed that the metal is in the  $z > 0$  half-space, and have denoted the MFP by  $\lambda(k)$ .

It should be noticed that<sup>15</sup> although Eq. (4) is essentially a one-body expression, many-body interactions are effectively included with the introduction of the damping of  $\phi^>$  [Eq. (6)]. In order to examine the validity of this expression, we obviously need to employ many-body theory; straightforward one-body consideration<sup>16,17</sup> is not appropriate to start with. Recently Almbladh<sup>18</sup> studied this problem and showed, via rigorous many-body perturbation theory, that the approach employed here is essentially correct (see Ref. 18 for details). Briefly speaking, Almbladh demonstrated that, first, the acceleration formalism [i.e., where the interaction  $H' \sim -\nabla \cdot V$ , as in Eq. (4)] satisfies the correct selection rule disregarding approximations made about the wave functions; second, the acceleration and the velocity formalisms (i.e.,  $H' \sim \mathbf{A} \cdot \mathbf{p}$ ) become equivalent only if proper vertex corrections are included in the latter. The acceleration formalism, freed from complicated vertex corrections, is, therefore, easier to apply. Almbladh also showed<sup>18</sup> the equivalence of Mahan's scattering theory,<sup>8</sup> which we use in the calculation, and other photoemission theories<sup>19</sup> based on the response formulation (i.e., the Kubo formula). This means that the results we obtained are very general, but with Mahan's theory, we gain the advantage to identify various effects easily.

The broadening of initial states was neglected in I, because the primary concern there were the stationary peaks in the gap, and the corresponding initial states are

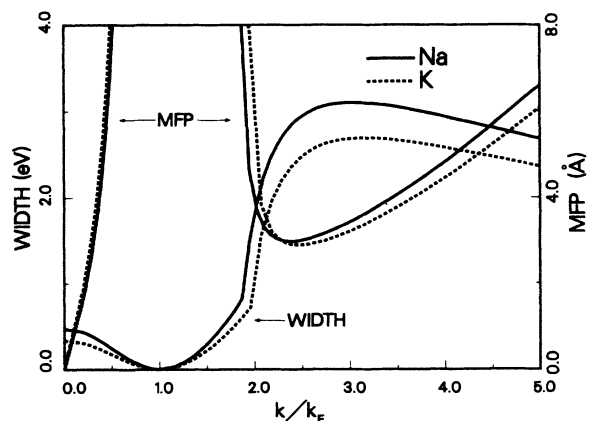


FIG. 2. The calculated electronic MFP and width [ $\Sigma_2(k)$ ] as a function of  $k$  are given for both Na and K.

sharp states close to  $E_F$  (see Fig. 2). Inclusion of the initial-state broadening effect can be most easily introduced in Eq. (3) by letting  $E(k_{i\perp})$  contain the imaginary part of the self-energy. As a result, the  $\delta$  function of Eq. (3) becomes a Lorentzian of width  $\Sigma_2(k)$ . More specifically, we can first express Eq. (3) in an equivalent form:

$$\frac{d^2 I}{d\Omega dE} = \frac{em}{2\pi^2} \int d\varepsilon p \langle \phi^>(p) | H' A(\varepsilon) H' | \phi^>(p) \rangle \times \delta(E \cos^2\theta - \varepsilon - \hbar\omega + V_0), \quad (3')$$

where  $A(\varepsilon)$  represents the spectral function of finding an electron at  $\varepsilon$ . When electronic interactions are neglected,

$$A(\varepsilon) = \sum_{k_i} |\phi(k_i)\rangle \langle \phi(k_i)| \delta(\varepsilon - E(k_i))$$

and we immediately recover Eq. (3). With the inclusion of the Coulomb scattering,  $A(\varepsilon)$  is broadened and can be described by a Lorentzian as we have just described. In Eq. (3') the energy is clearly conserved in the process. This can be compared with the no-loss (no energy loss to the system) spectrum of Almladh.<sup>18</sup> All the calculations presented in this work contain the initial-state broadening effect. Although this broadening effect is not important in the gap region, it is found to have an important bearing on the observed bandwidth, as we will see shortly.

The procedure of calculation is, first, to determine the wave functions  $\phi$  and  $\phi^>$  with LK's surface potential,<sup>12</sup> and then, to modify  $\phi^>$  according to Eq. (6). The wave functions are subsequently used to evaluate  $M(p, k_i)$  in Eq. (4), and finally the spectrum via Eq. (3). It is in the last step where the initial-state broadening is incorporated. The calculation is numerically straightforward. We only need to specify the electron density ( $r_s$ ) (Ref. 20) and the crystal potential; the latter can be described by Ashcroft's pseudopotential ( $r_c$ ).<sup>21</sup> All the calculations, including that of the LK surface potential and that of the self-energy, are completely determined once  $r_s$  and  $r_c$  are given. In Table I we give the values of  $r_s$ ,  $r_c$ , and  $V_G$ , for both Na and K, that are used in this work. There are concerns<sup>17,22</sup> over the signs of  $V_G$ , which we shall discuss further in Sec. IV. The results of our calculation are presented in the next section.

TABLE I. Parameters used in the calculation.  $r_s$  (the electron density) and  $r_c$  (the Ashcroft pseudopotential radius) are expressed in atomic units. The crystal potentials  $V_G$  are in eV.

	$r_s^a$	$r_c^b$	$V_{110}^c$	$V_{220}^c$
Na	3.93	1.664	0.296	0.2296
K	4.86	2.14	0.1515	0.0833

<sup>a</sup> Reference 15.

<sup>b</sup> Reference 16.

<sup>c</sup> This calculation.

### III. CALCULATED RESULTS AND DISCUSSIONS

Figures 3 and 4 demonstrate the calculated spectra at two photon energies representing the cases in and around the expected gap. These calculated spectra differ from our earlier results<sup>6</sup> by having included the initial-state broadenings, i.e.,  $\Sigma_2(k_i) \neq 0$ . The thin, solid curves represent diagonal terms from various effects, as indicated. Interference between these effects (the dashed-dotted curves) is obviously strong and important. The heavy solid curves are unbroadened spectra which, after being convoluted by a Gaussian of 0.3 eV in width for instrumental resolutions,<sup>3</sup> are shown by the dashed curves. These broadened spectra can be directly compared with JP's measurement. We iterate that the calculations here contain the initial-state broadening effect which was neglected in I. Although the general features of the spectra are not affected by this extra broadening factor, the detailed structures (e.g., the peak positions) are modified, as we shall examine in greater detail later in this article.

It has been pointed out in I that the edge structure at  $E_F$  (Fig. 3) and the stationary, narrow peaks in the gap region (Fig. 4) actually come from the same physical origins: (a) The final states are broad (see Fig. 2)—a fact that makes nonvertical transitions important, and (b) the initial states at the Fermi level are very sharp. In cases when vertical transitions are possible (Fig. 3), the sharp cutoff at  $E_F$  causes a similar structure (i.e., the edge) in

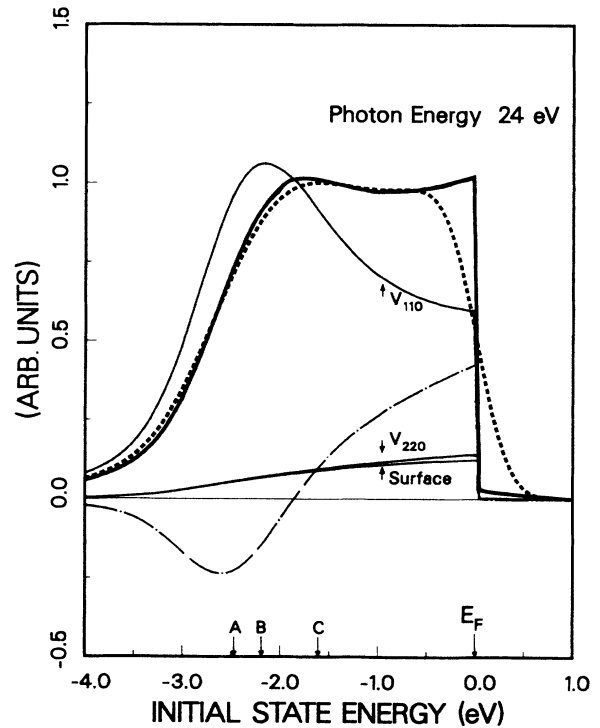


FIG. 3. The calculated spectrum at  $\hbar\omega = 24$  eV is shown by the heavy solid curve. After the inclusion of the instrumental resolution, the result is shown by the dashed curve. The thin solid curves are diagonal terms from various bulk and surface effects, as indicated. An interference term is plotted by the dashed-dotted curve.

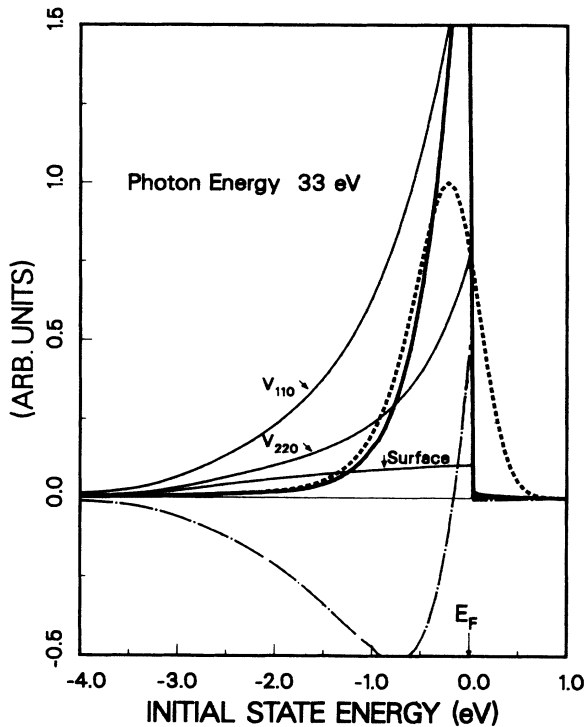


FIG. 4. This is the same plot as Fig. 3, but for  $\hbar\omega=33$  eV. The transition would be forbidden if the final-state broadening were neglected (see Fig. 1).

the spectra. In cases when vertical transitions are forbidden (Fig. 4), nonvertical transitions become the dominant constituent in the spectra and the cutoff at  $E_F$  causes "narrowed" peaks at the Fermi level (see also Fig. 1). These features are clearly illustrated in the calculated spectra, which provide an explanation to the observed edge structure at  $E_F$ .<sup>3</sup>

In support of the reasoning given above, we would like to point out that similar edge structures at  $E_F$  are also found in the spectra of Al (Ref. 1) and Mg (Ref. 4). These structures can be easily understood according to the same arguments which we give for Na. In the normal-emission spectra of Be(0001),<sup>2</sup> however, there is no structure at  $E_F$ . This result is consistent with our theory since the Fermi level passes through an energy gap<sup>2</sup> in Be(0001) and, hence, the edge structure is absent from the spectra. From this experimental evidence, it seems reasonable for us to conclude the following: The edge structure at  $E_F$  is a general feature in photoemission spectra provided that there are occupied states at the Fermi level and that the final states are sufficiently broad (see Fig. 1).

As to the peaks in the gap regions, our theory predicts that their strength and width should both be reduced. These effects can be understood by using Fig. 1 and noticing that transitions corresponding to  $k > k_F$  are suppressed. The calculated results of Na and K are shown in Fig. 5, which clearly demonstrates the property that both the peak intensity and the peak width are reduced in the gap. It should be noted that, at energies

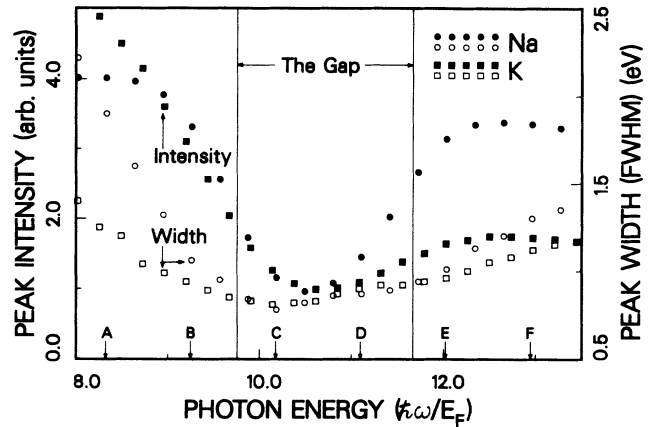


FIG. 5. The calculated peak intensities (the solid marks) and the peak widths (the open marks) around the gap region are shown. The gap location remains the same for both Na and K (and also other alkali metals) when we express  $\hbar\omega$  in units of  $E_F$ . *A, B, . . . , F* indicate photon energies for which we have studied the angle dependence of the spectra, and the results are given in Fig. 6.

away from the gap region it is the Fermi-level intensity that is given in Fig. 5, and the width is determined by the positions where intensities fall to half the Fermi-level value. This procedure is reasonable, since our main concern here is only at the gap region. The difference between Na and K in the peak intensity at  $\hbar\omega \sim 12E_F$  is due to the fact that  $V_{220}$  is weaker in K than in Na (see Table I). Actually, since all alkali metals have very similar band structures, they should, according to our theory, have similar features in the photoemission spectra (e.g., the edge and the stationary peaks at  $E_F$ ).

The angle-dependent behavior of the spectra is also of interest, and near-normal-emission spectra can be easily evaluated with Eq. (3). It was noted in I that the persistence of the peaks in the gap region depends critically on the closeness of the band edge and the Fermi level—a condition which was summarized by Eq. (4) of I for normal-emission spectra. A similar relation for prominent peaks in the gap region in near-normal emission reads

$$\frac{1}{2}G_{110} - k_{m\perp} \leq \lambda^{-1}(p), \quad (7)$$

where  $k_{m\perp}$  was defined by Eq. (3). As the emission angle ( $\theta$ ) increases, this relation becomes less well satisfied and the peak strength in the gap region gets weaker accordingly. On the other hand, vertical transitions are not as strongly angle dependent since these transitions do not rely on the broadness of the final states. Figure 6 demonstrates the sensitive angle dependence of the peaks in the gap (*C* curves), which contrast sharply with those peaks from vertical transitions (*A* curves) also shown in the figure. Peaks that are outside of, but close to, the gap region (*B* curves) show intermediate angle dependence. We have also calculated the angle-dependent spectra at photon energies that correspond to *D, E,* and *F* marked in

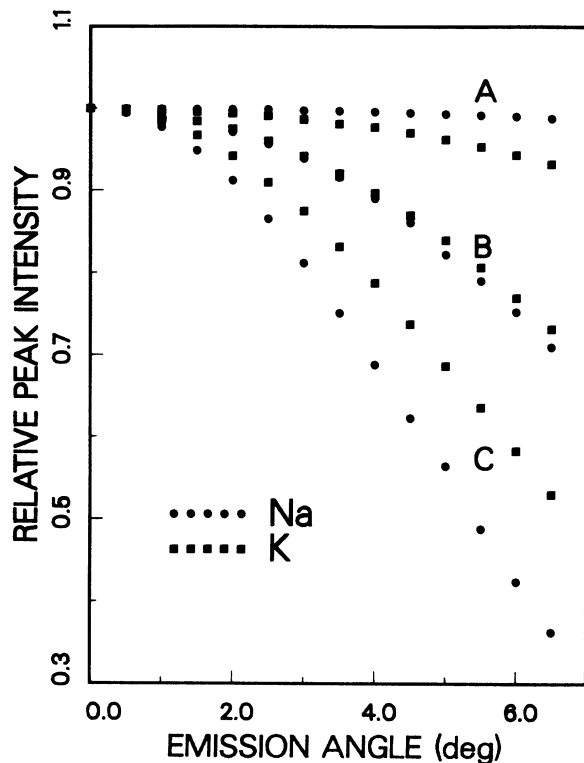


FIG. 6. The angle dependence of the spectrum intensity (the peak height) at three chosen photon energies are shown; the photon energies *A*, *B*, and *C* are defined in Fig. 5. The angle dependence is strong for the peaks inside the gap and becomes weaker when we move away from the gap region. Similar results are found for photon energies at *D*, *E*, and *F* of Fig. 5.

Fig. 5. The results are completely analogous to those shown in Fig. 6, with an angle dependence varying according to relative displacement of the energy from the gap region. Again, the behavior of Na and K is found to be similar because of their similar band structure. We expect this angle-dependent behavior to be common to all alkali metals because of their similar band structures.

We now proceed to discuss the band structure of simple metals. From photoemission spectra, we can determine the band by plotting the peak positions versus the photoenergies, as shown by Fig. 7 from the results of Na. The solid curve in the figure is a NFE band that satisfies Eq. (1), the crosses are from JP's measurement, and the dotted curve from our calculation. We notice that, despite a general agreement on the shape of the band, these results differ noticeably both at  $E_F$ , and at the bottom of the band.

The stationary peaks in the gap, which we discussed earlier, form a bridge that connects the two separate branches of the NFE model. Both our calculation and the measurement agree that the bridge is shifted downward from  $E_F$  for  $\sim 0.23$  eV, due to the effect of the instrumental broadening (see Fig. 4).

In JP's measurement,<sup>3</sup> there are some electron-energy distributions at high-photon energy which show two

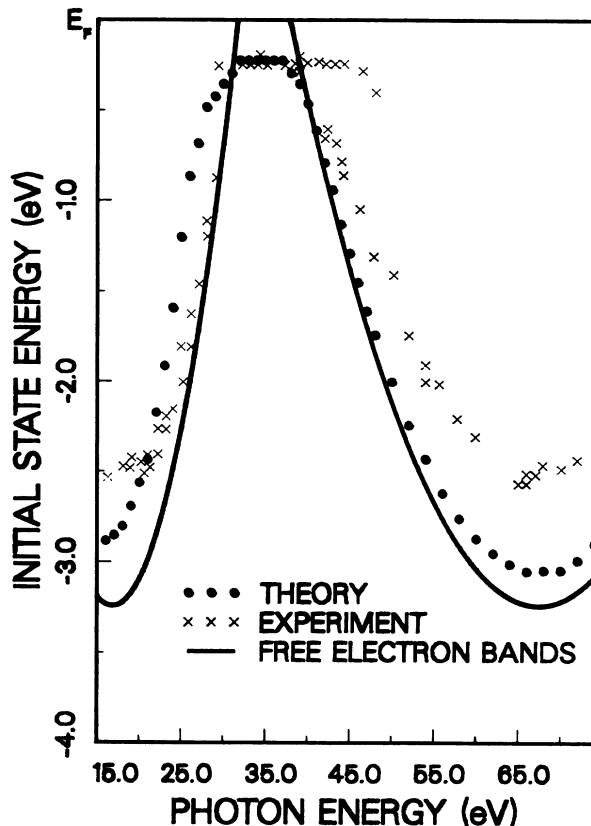


FIG. 7. We compare the calculated and the measured peak position as a function of the photon energy. In the calculation, the broadenings of both the initial and the final states are included. Both the theoretical points and the experimental data contain the instrumental broadening effect.

peaks: one near the direct transition and one near  $E_F$ . Our theory does not explain this second peak near the Fermi energy. In fact, these extra peaks are a mystery and are not predicted by any theory. Overhauser claims that they are explained by his theory of CDW.<sup>16,17</sup> However, he has not published any calculated spectra which show this peak, so his claim is unsubstantiated. Kaiser, Inglesfield, and Aers<sup>23</sup> have suggested that this extra peak is due to a surface resonance located  $\sim 0.75$  eV above the Fermi energy, but their calculated spectra also do not show a peak. As we said, this second peak is still unexplained by any theory.

Figure 7 also demonstrates that the band from our calculation is narrower than the NFE band by 0.2–0.4 eV—most noticeably at the bottom of the band. This bandwidth narrowing is mainly due to the broadening of the initial states and is clearly illustrated by Fig. 3. The marker *A* therein indicates the peak position if Eq. (1) is satisfied, i.e., from a vertical transition between the NFE bands. After the broadenings are included, the peak position of the “vertical transition” appears at *B*, which is  $\sim 0.3$  eV higher than *A*. The shift of the peak position is due to the fact that electron states at the band bottom are much broader (i.e., the corresponding transitions become

more dispersed) than shallower states (see Fig. 2). Interference and the instrumental broadening further modify the spectra and, as a result (which is shown in Fig. 3), the final peak position is at C. Our calculation, therefore, clearly demonstrates two intrinsic effects in photoemission that could appreciably affect the peak positions: the broadening of electron states and the interference.

Let us look at the interference term first. When the photon energy is not close to the gap region, interference is mainly due to the mixing between the surface and the bulk term that corresponds to the vertical transition. Therefore, when the surface contribution is not negligible compared with the bulk term, we usually find strong interference; for example, Fig. 3. We thus need to keep the surface term small to minimize the interference effect. We find that the surface contribution decreases as the photoenergy increases. As the emitted electron becomes more energetic, the final state has more oscillations in the surface region and hence causes a larger cancellation in the surface term. It is due to this fact that our calculated results agree better with the NFE band at higher photon energies (Fig. 7). The results suggest that the band structure can be better determined by photoemission with energetic photon sources.

The modification of the bandwidth is mainly due to the initial state broadenings and not to the interference. In order to determine the band size we need to locate the bottom of the band. The surface effect, and hence the interference, is small for those states at the band bottom. In regards to the size of modification due to the initial-state broadening, we find that it decreases as the slope of the final-state band  $dE(k)/dk$ , increases, i.e., as the final states become more energetic. As a result, our calculation shows different bandwidth change (to be denoted by  $D_1$ ) at  $\hbar\omega=16$  eV ( $D_1=-0.36$  eV) and  $\hbar\omega=75$  eV ( $D_1=-0.19$  eV). This kind of broadening effect should always be taken into account when the band under consideration is sufficiently wide that the electron width differs a great deal from the bottom of the band to the top. Since this is generally the case for simple metals, it comes as no surprise that the measured conduction-bandwidths usually appear narrower than that from band-structure calculations,<sup>1,3,4</sup> with the exception of Be.<sup>2</sup> But by considering the effect that  $D_1$  decreases as  $\hbar\omega$  increases, we expect the conduction band of simple metals to be better determined with more energetic photon sources. We remark that it is difficult to tell from JP's results<sup>3</sup> if the measured bandwidth actually varies with  $\hbar\omega$ , because of the large instrumental resolution ( $\sim 0.3$  eV).

There are other effects that could modify the bandwidth. Because of the Coulomb interaction, electron states must be renormalized. This is a many-body effect which modifies the bandwidth by an amount  $D_2 = \Sigma_1(k=0) - \Sigma_1(k_F)$ , where  $\Sigma_1$  is the real part of the self-energy introduced by Eq. (5). There is also the effect of the crystal potential which modifies the band structure and shifts the Fermi level by an amount  $D_3$ . In Table II we summarize all these bandwidths-narrowing effects for the metals of Na and K. The total of these effects amounts to a large bandwidth reduction: 0.63–0.80 eV

TABLE II. Various bandwidth-narrowing factors are listed below. All values are in eV. Negative values signify a reduction in bandwidth.  $E_F$  is the NFE bandwidth.

	$E_F$	$D_1^a$	$D_2^b$	$D_3^c$
Na	3.24	-0.19 to -0.36	-0.38	-0.06
K	2.12	-0.18 to -0.25	-0.34	-0.07

<sup>a</sup> This calculation.

<sup>b</sup> Reference 13.

<sup>c</sup> Reference 8.

for Na and 0.59–0.66 eV for K. The result of Na is surprisingly close to JP's measurement, which reports a narrowing of  $0.7 \pm 0.1$  eV. We note that a large bandwidth reduction in K has also been observed ( $\sim 0.7$  eV).<sup>24</sup> Probably the quantitative agreement should not be overemphasized in view of the many approximations that have been employed in the calculation. Additionally, there exists some difference in the size of  $D_2$  between the calculation of Ref. 12 and others'.<sup>25</sup> However, the deficiency is not likely to offset our conclusion, which is that the large bandwidth narrowing of Na is partly caused by the many-body effect and is partly due to the limitation inherent in low-energy photoemission processes.

Similar reductions in the bandwidth are expected for other simple metals. The results of Na and K show that the effect (i.e.,  $D_1$ ) is roughly of the size  $\Sigma_2(k=0)$ . Therefore, this effect could be more prominent for multivalent simple metals [e.g.,  $\Sigma_2(k=0)$  is 0.87 eV (1.27 eV) for Mg (Al)]. Meanwhile, it should be reemphasized that, as we argued earlier, the bandwidth reduction due to the initial-state broadening decreases as the photon energy is increased. In order to examine these effects closely, detailed calculations (with both  $\Sigma_1$  and  $\Sigma_2$  included) and measurements are needed.

#### IV. NEW MEASUREMENTS AND FURTHER DISCUSSIONS

After the present calculation was first completed, new measured results on Na were made available to us by Plummer and Lyo.<sup>9</sup> It seems plausible to include these new data in this paper and to compare them with our calculations. We will do so in the following, together with a discussion on the sign of the crystal potentials and a comment on CDW's in simple metals.

In the new photoemission studies of Plummer and Lyo, the width, the strength, and the angle dependence of the peaks in the gap region are measured. The new results also reflect an improvement in instrumental resolution (0.05 eV in FWHM). The predicted decreases in the peak width and its strength (Fig. 5), and the sensitive angle dependence (Fig. 6), are observed, but some discrepancies exist between our calculations and the new measurements (see below).

In the comparison with Fig. 5, the measured results show that the decreases in width and in intensity appear at photon energies  $\sim 3$  eV higher than from our calculation, suggesting that the gap is actually at a higher energy than the NFE gap. We believe that this energy shift is

due to the self-energy corrections, i.e., due to the real part of  $\Sigma(p)$  of Eq. (5). Calculations that incorporate with the self-energy shifts will be discussed elsewhere.<sup>26</sup> The new measurement, which has better resolution, shows that the peaks in the gap are as narrow as  $\sim 0.35$  eV in full width, which is much narrower than 0.8 eV of Fig. 5 and of JP's original measurement.<sup>3</sup> We find in our recent calculation that if 0.05-eV resolution is used, we also obtain a very narrow peak of about 0.35 eV in width.<sup>26</sup> Actually, it can be easily seen from Fig. 4 that the observed peak width (dashed curve) is mainly due to instrumental broadenings.

The measured<sup>9</sup> angle dependence of peak intensities in the gap region are shown in Fig. 8, where the calculated results of Fig. 6 (solid circles denoted by *B* and *C*) are also included for comparison. The measurements are made in the directions that are parallel to the plane of the incident light (even) and perpendicular to it (odd). At  $\hbar\omega = 40$  eV, which is above the upper edge of the gap (of NFE bands), the results are expected to follow the *B* curves, while at  $\hbar\omega = 35$  eV, which is at the center of the gap, the results are to follow the *C* curves which decrease much more rapidly as the angle increases. However, the measured results at the two photon energies have similar angle dependence which lies somewhere between the *B* and *C* curves. This result can be explained in accordance with the self-energy shifts in the following way. If we rigidly shift the gap upward for  $\sim 3$  eV,  $\hbar\omega = 35$  and 40 eV would be at the lower and upper edge of the gap, respectively. Then, the angle dependence at these photon ener-

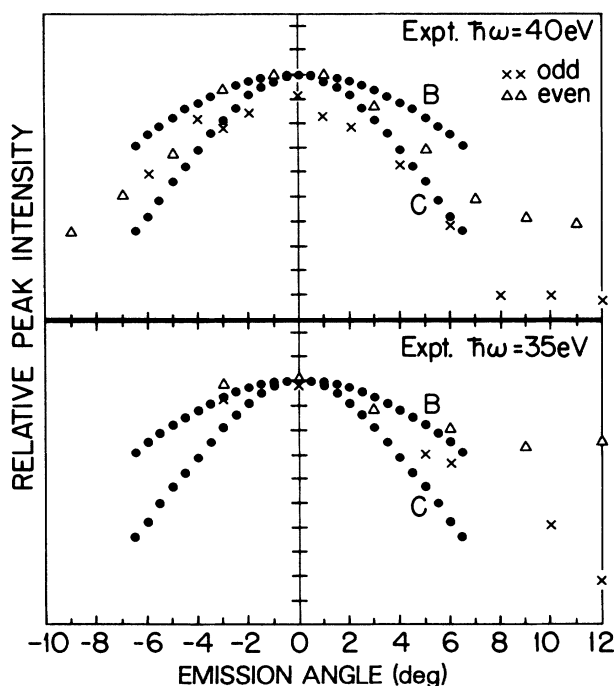


FIG. 8. The measured angle dependence of peak intensities at  $\hbar\omega = 35$  and 40 eV. Crosses (odd) denote measurement made in the direction perpendicular to the plane of light and triangles (even) that parallel to it. Calculated results (solid circles) marked by *B* and *C* are the same as in Fig. 6.

gies should, indeed, be similar. Taking this viewpoint, we expect that a more dramatic dependence on the emission angle to be observed at  $\hbar\omega = 37$ –38 eV.

The measured results of Fig. 8 demonstrate an important feature which our present calculation cannot explain. Namely, there is obvious azimuthal-angle dependence in the measurement (i.e., differences between the odd and the even curves, most notable at large emission angles at  $\hbar\omega = 35$  eV), but Eqs. (3) and (4) of our calculation do not depend on the azimuthal angle. However, it should be emphasized that full predictions of the NFE model,<sup>8</sup> in fact, do allow azimuthal-angle dependence, which is discussed below.

Equations (3) and (4) only include the primary cones<sup>8</sup> of  $G_{110}$  and  $G_{220}$  which are normal to the surface and, hence, suggest that the spectra are symmetric about the *z* axis. However, there are many secondary cones due to primary *G* vectors which are not normal to the surface. The surface Bragg reflection can scatter some of these electrons into an exit trajectory, and azimuthal-angle dependence is therefore possible. Figure 9 demonstrates our calculated primary cones (solid curves) and secondary cones (dashed curves) for the Na(110) surface at  $\hbar\omega = 18$  eV. These are found using the formulas in Mahan's paper.<sup>8</sup> This figure may not include all secondary cones since we only took a few primary *G* vectors, although we took all possible values of *G* parallel for the Bragg reflection at the surface. At higher photon energies, more secondary cones would appear since more combinations of the *G* vectors are possible. But even at  $\hbar\omega = 18$  eV the secondary cones already introduce complicated dependence on the azimuthal angle of photoelectrons.

We choose  $\hbar\omega = 18$  eV for demonstration for the reason that Plummer and Lyo have measured the spectrum at this energy and found<sup>9</sup> strong angle dependence, especially near  $26^\circ$ – $27^\circ$  from normal. From Fig. 9 we notice that a lot is happening at these angles. There the main primary cone terminates, some secondary cones terminate, while other secondary cones start. This may

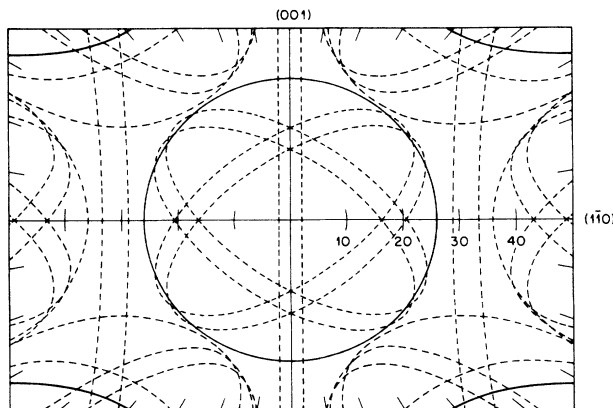


FIG. 9. A demonstration of our calculated primary cones (solid lines) and secondary cones (dashed lines) for the Na(110) surface at  $\hbar\omega = 18$  eV. The polar angles are given in degrees.

qualitatively explain the observation of Plummer and Lyo regarding the dramatic change in the spectra at this angle and photon energy. We further remark that the secondary cones predict a dependence on the azimuthal angle in photoemission even for electrons near the normal direction. The nearly straight lines which come within  $2^\circ$  of normal are secondary cones for a primary  $G$  vector which is parallel to the surface plane. This  $G$  vector gives no external primary cones, but is responsible for the nearly straight lines as secondary cones.

In brief, the new measurements of Plummer and Lyo suggest to us that the self-energy shift is important in the problem. We have found much improved agreement with the new results when the self-energy corrections are fully taken into account, and details of that calculation will be given elsewhere.<sup>26</sup> In addition, measurements of Plummer and Lyo show that photoemission spectra are azimuthal-angle dependent. Although this azimuthal-angle dependence cannot be explained with the present formalism [Eqs. (3) and (4)], we have demonstrated that it may possibly be caused by surface Bragg reflection (i.e., the secondary cones), which is predicted within the NFE model. In what follows, we will discuss the sign of crystal potentials.

After our calculation was first published,<sup>6</sup> Overhauser questioned<sup>17</sup> the sign of the lattice potential  $V_{110}$ , which appears in Eq. (4). He argues that  $V_{110}$  should be negative for both K (Ref. 22) and Na (Ref. 17) and not positive as we have used in the calculation. The sign of this lattice potential is important since if it changes so would the interference term (see Fig. 3), and the edge structure at  $E_F$  would be much weaker as a result. However, most calculations find that  $V_{110}$  is positive, contrary to Overhauser's claim.

We notice that there is another factor which could modify the sign of crystal potentials. Namely, the distance ( $d$ ) between the surface layer of ions and the jellium edge.<sup>12</sup> In our calculation, where we set  $V_c(z) = \sum_G V_G \exp(-iGz)$ ,  $d$  is equivalent to zero. It is more reasonable<sup>12</sup> to set  $d = c/2$ , where  $c$  is one-half the distance between two adjacent ion layers. By including this factor, we would get

$$V_c(z) = -V_{110} \exp(-iG_{110}z) + V_{220} \exp(-iG_{220}z),$$

i.e., an extra minus sign is introduced to the  $V_{110}$  term.

As we have explained, changing the sign of  $V_{110}$  in our calculation would significantly reduce the size of the edge structure at  $E_F$  and, hence, cause discrepancies if compared with the measurements. The close agreement between our calculated results and the measurements seems, therefore, a strong indication that this extra sign due to  $d = c/2$  is cancelled. One possibility of this cancellation is that  $V_{110}$  is indeed negative—as Overhauser has claimed; although we are not aware of independent verifications on negative  $V_{110}$ . We remark that we have also let  $d$  vary by up to 10% of  $c/2$  and find no appreciable change in the spectra—demonstrating that effects due to possible surface relaxations<sup>12</sup> are of minor importance in the problem of photoemission.

Lastly, we would like to comment on the existence of

CDW's in simple metals. In a model calculation, Overhauser<sup>5</sup> introduced a periodic potential  $V_{CDW}(a) = \sum_Q V_Q e^{-iQz}$  due to the presence of CDW's, where  $Q = \pm 2k_F$ . This extra potential would severely distort the conduction band at  $E_F$  and hence could also explain the stationary peaks found in JP's experiment. However, according to the arguments that lead to Eq. (4), this potential from CDW must also induce photoexcitations. Stated more precisely, there should be peaks in the spectra at positions (roughly) determined by

$$E(\mathbf{k} + \mathbf{Q}) = E(\mathbf{k}) + \hbar\omega. \quad (8)$$

These peaks are, in addition to those induced by the lattice potential [i.e., determined by Eq. (1)], not from a fixed  $E(\mathbf{k})$  (i.e., not stationary). Then, at a given photon energy, there should always have two peaks in the spectra,<sup>27</sup> but it is basically a single-peak structure in accordance with Eq. (1) that was observed experimentally. From this observation, we are able to conclude that the CDW, if it exists at all in Na, must be a very weak one. It can be seen readily that the large  $V_Q$  (more than twice as large as  $V_G$ ), which Overhauser uses to account for the stationary peaks in the gap, is not a realistic one for Na.

The foregoing discussions, concerning both the photoemission spectrum of Na, and its relation to the CDW's in the system, can be applied to other simple metals as well. It should be revealing to look for, experimentally, peaks that are induced by the CDW potential [i.e., Eq. (8)], since this is a very direct way to see if a CDW exists in the system at all.

## V. CONCLUDING REMARKS

We have performed a calculation which is based on the photoemission theory of Mahan.<sup>8</sup> In the calculation, various surface and bulk effects are included. The results show that the peak positions generally agree with the prediction of Eq. (1), i.e., the NFE model, to within the broadness of the electron states. The importance of the decaying factors for electrons is that they open up channels for nonvertical (or momentum-nonconserving) excitations. Due to the effect of broad states, our calculated results reproduce the important features which were found experimentally: (a) there appears an edge structure at  $E_F$  in the spectra, (b) there are stationary peaks in the gap region, and (c) the bandwidth is reduced. The close agreement between the theory and the measurement is a strong indication that a NFE band is valid for the system. This calculation also suggests that the conduction band of simple metals can be more accurately measured with photoemission experiments using higher-energy photon sources, since both the interference and the initial-state broadening effect on the bandwidth are reduced at higher energies.

In this paper, we have also discussed new experimental results of Plummer *et al.*, where the angle dependence is measured and better resolution is achieved. By comparing our calculation with the measurement, we argue that

the self-energy shifts of the electron states are important in the problem. Details of this self-energy correction will be discussed in a separate paper.<sup>26</sup> We have also shown the importance of surface Bragg reflection, which causes many secondary cones—an effect could possibly account for the azimuthal-angle anisotropy observed by Plummer and Lyo. The importance concerning the sign of  $V_{110}$  is also addressed, where some confusion still remains. Finally, we comment on the CDW's and argue that photoemission measurement should provide us with direct evidence on whether CDW's exist in the system. Obviously, more photoemission studies, on both the theoretical and the experimental sides, are needed to unveil the not necessarily simple properties of the so-called simple metals.

#### ACKNOWLEDGMENTS

The authors thank Dr. D. R. Hamann, Dr. E. W. Plummer, and Dr. B. E. Sernelius for helpful conversations; they also thank E. W. Plummer and I.-W. Lyo for providing them with unpublished data. This research was sponsored jointly by the National Science Foundation through Grant No. DMR-85-01101, by the University of Tennessee, and by the Division of Materials Sciences, U.S. Department of Energy, under Contract No. DE-AC05-8421400 with Martin Marietta Energy Systems, Inc. One of the authors (K.S.) is thankful for the support of the National Science Foundation through Grant No. DMR-85-05474 through the University of Michigan.

\*Present address: Department of Physics, University of Michigan, Ann Arbor, MI 48109.

<sup>1</sup>H. J. Levinson, F. Greuter, and E. W. Plummer, *Phys. Rev. B* **27**, 727 (1983).

<sup>2</sup>E. Jenson, R. A. Bartynski, T. Gustafsson, E. W. Plummer, M. Y. Chou, M. L. Cohen, and G. B. Hoflund, *Phys. Rev. B* **30**, 5500 (1984).

<sup>3</sup>E. Jensen and E. W. Plummer, *Phys. Rev. Lett.* **55**, 1912 (1985).

<sup>4</sup>R. A. Bartynski, R. H. Gaylord, T. Gustafsson, and E. W. Plummer, *Phys. Rev. B* **33**, 3644 (1986).

<sup>5</sup>A. W. Overhauser, *Phys. Rev. Lett.* **55**, 1916 (1985).

<sup>6</sup>K. W.-K. Shung and G. D. Mahan, *Phys. Rev. Lett.* **57**, 1076 (1986).

<sup>7</sup>L. Hedin and S. Lundqvist, in *Solid State Physics*, edited by H. Ehenreich, F. Seitz, and D. Turnbull (Academic, New York, 1969), Vol. 23, p. 1.

<sup>8</sup>G. D. Mahan, *Phys. Rev. B* **2**, 4334 (1970).

<sup>9</sup>E. W. Plummer and I.-W. Lyo (private communication).

<sup>10</sup>See, for example, G. D. Mahan, *Many-Particle Physics* (Plenum, New York, 1981).

<sup>11</sup>R. Kammerer, J. Barth, F. Gerken, C. Kunz, S. A. Flodström, and L. I. Johansson, *Phys. Rev. B* **26**, 3491 (1982).

<sup>12</sup>N. D. Lang and W. Kohn, *Phys. Rev. B* **1**, 4555 (1970).

<sup>13</sup>B. Sernelius (private communication).

<sup>14</sup>J. J. Quinn, *Phys. Rev.* **126**, 1453 (1962).

<sup>15</sup>K. W.-K. Shung and G. D. Mahan, *Phys. Rev. Lett.* **58**, 960 (1987).

<sup>16</sup>P. J. Feibelman, *Surf. Sci.* **46**, 558 (1974).

<sup>17</sup>A. W. Overhauser, *Phys. Rev. Lett.* **58**, 959 (1987).

<sup>18</sup>C.-O. Almbladh, *Phys. Scr.* **32**, 341 (1985); *Phys. Rev. B* **34**, 3798 (1986).

<sup>19</sup>See Ref. 17.

<sup>20</sup>N. W. Ashcroft and N. D. Mermin, *Solid State Physics* (Holt, Rinehart and Winston, New York, 1976).

<sup>21</sup>N. W. Ashcroft, *Phys. Lett.* **23**, 48 (1966).

<sup>22</sup>A. C. Tselis and A. W. Overhauser, *Phys. Rev. Lett.* **54**, 1299 (1985).

<sup>23</sup>J. H. Kaiser, J. E. Ingelsfield, and G. C. Aers, *Solid State Commun.* **63**, 689 (1987).

<sup>24</sup>J. Song, E. Jensen, and E. W. Plummer (unpublished).

<sup>25</sup>From Ref. 7,  $D_2$ 's are  $-0.27$  and  $-0.24$  eV for Na and K, respectively. These values differ by  $\sim 0.1$  eV from our calculations. (See Ref. 12.) We note that  $D_2$  is the difference between two large numbers (i.e.,  $\Sigma_1 \sim 5$  eV); hence, differences between the two approaches in calculating the self-energy are exaggerated in the value of  $D_2$ .

<sup>26</sup>K. W.-K. Shung, B. E. Sernelius, and G. D. Mahan, *Phys. Rev. B* **36**, 4499 (1987).

<sup>27</sup>Actually, if the CDW's exist in the system, we should observe more than two peaks in the spectra. This is because the conduction band becomes a set of many minibands due to the two periodic potentials  $V_c(z)$  and  $V_{CDW}(z)$  in the system (see Fig. 4 of Ref. 5). We can imagine that these minibands are evaluated by  $\hbar\omega$  due to the photon excitation and that the peaks are a result of their intersection with the empty bands. There would be many intersections and hence many peaks in the spectra; those satisfying Eqs. (1) and (8) are the leading terms in powers of  $V_Q$  and  $V_G$ .

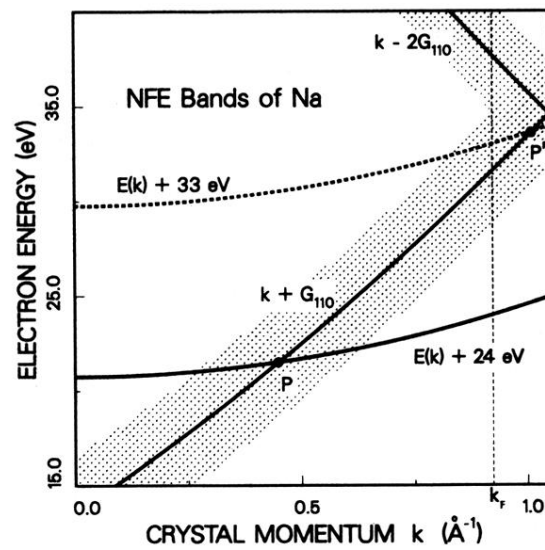


FIG. 1. The NFE bands of Na are shown in which the conduction band has been elevated by the applied photon energies of 24 eV (the solid curve) and 33 eV (the dashed curve), respectively. The intersections  $P$  and  $P'$  correspond to the vertical transitions in photoemission at the given photon energies. The shaded curves represent the broadened final states.